Journal of Engineering Sciences

Vol 12, Issue 07, July/2021
ISSN NO:0377-9254

# Single Phase Single Stage Grid - Connected Photovoltaic System Using enhanced H6 Topology

[1]P Yoga Bhavishya, UG Student, Department of EEE, Pragati Engineering college, Surampalem, bhavishyaparuchuri99@gmail.com

[2]P Venkata Sai Nikitha, UG Student, Department of EEE, Pragati Engineering college, Surampalem, nikithapasupuleti24@gmail.com

[3]Perla Amulya, UG Student, Department of EEE, Pragati Engineering college, Surampalem, amulyaperla30@gmail.cok

[4]P S V L Suneetha, UG Student, Department of EEE, Pragati Engineering college, Surampalem, peta.suneetha2016@gmail.com

[5]Rampa Shalini, UG Student, Department of EEE, Pragati Engineering college, Surampalem, shalusmile999@gmail.com

**Abstract:** grid feeding solar photovoltaic (PV) inverters to suppress the second harmonic and switching frequency voltage ripples. With aging equivalent series resistance (ESR) of capacitor increases and its capacitance value decreases, which lead to increase in dc-link voltage ripple Oscillations in PV operating point around its maximum power point (MPP), results in reduction of average output power and revenue generated. To address this, frequent replacement of capacitors are required, which may lead to increased cost. Therefore, capacitors must be replaced at an optimal period to ensure maximum earnings. To realize this, a technique for monitoring of power extraction efficiency (PEE) is proposed in this paper. Further, criteria for replacement of capacitor based on the measured values of PEE are suggested. Mathematical model relating the capacitance and ESR values to the PEE is derived. Effect of variation in temperature and solar radiation on PEE is discussed. Detailed simulation studies are carried out using MATLAB Simulink. A scaled down laboratory prototype of inverter is developed. The proposed technique is implemented in the existing digital processor/controller used for MPP tracking, thereby avoiding additional circuits/sensors.PEE estimated by simulation and experimentation are found to be within 1% of each other.

## I. INTRODUCTION

Power electronic inverters are used to integrate solar photovoltaic (PV) with grid [1]. Power fed to the grid from the PV system is affected by 1) efficiency of PV panels, 2) conversion losses in the inverter, and 3) power extraction efficiency (PEE). Efficiency of the PV panel is dependent on the material used and the manufacturing process. Second factor is the conversion losses in the inverter, which includes switching and conduction losses. Third factor affecting the output power is the PEE of solar inverter. This parameter is defined as the ratio of average power extracted from PV panel by the inverter to the maximum possible power available from the PV panel. Extraction efficiency decreases due to oscillations in PV voltage around the maximum power point (MPP). These oscillations are due to:1) maximum power point tracking (MPPT) algorithm, and 2)dc-link voltage ripple (of twice the grid frequency) in the case of a single phase inverter. Typically, extraction efficiency due to various MPPT algorithms may vary between 90% and 99%[2]–[4] and is not affected by the aging of capacitor. Second factor affecting the extraction efficiency in single phase PV inverters is the oscillations in dc-link voltage of twice the grid frequency [5]. To suppress these oscillations, electrolytic capacitors are popularly used due to their low cost and volume as compared to film-type capacitors [6]. However, electrolytic capacitor degrades due to its electrolyte loss with time, which leads to rise in equivalent series resistance (ESR) and fall in capacitance value [7]. Further, the rate of loss in electrolyte increases with high operating temperature of the solar inverter. The increase in the ESR value and the decrease in capacitance lead to the increase of oscillations in PV voltage. This leads to the increase in power oscillations around its MPP, thereby reducing the PEE and available output power from the inverter[8], [9]. In summary, due to aging capacitance reduces and ESR increases, which reduces the PEE and available output power.

This leads to the decrease in the earnings from the PV system. Therefore, timely replacement of electrolytic capacitor is desired. Various techniques are discussed in the literature for online health monitoring of electrolytic capacitors used in dc–dc converters[10]–[13] and inverters [14]–[22]. In [14], the ratio of average power loss in electrolytic capacitor to the square of root mean square (RMS) of current flowing through capacitors evaluated to determine ESR. If this value exceeds predefined limit, appropriate replacement of capacitor is indicated. To implement this technique, dedicated analog ICs are used to find the RMS of capacitor current and voltage. To avoid the use of dedicated analog ICs, another technique based on the power loss of capacitor is suggested in [15]. In this, the RMS of capacitor current is calculated using digital controllers with high sampling rate. Both the techniques [14], [15] require measurement of capacitor current for which a current sensor is placed deteriorate the capacitor voltage waveform as discussed in [13].To avoid high sampling rate and additional dc-link current sensor, techniques are suggested in [16]–[19]. These techniques estimate capacitance and/or ESR based on the low frequency measurements. A sub harmonic external ac current is injected from the source side due to which ripples are produced across dc-link capacitor. Capacitor current is reconstructed by using line currents and switch states of the inverter. Thereafter, the recursive least-squares method is used for the estimation of ESR or capacitance [16]–[19]. In [20], an external voltage at low frequency is injected in the

dc-link capacitor and the support vector regression (SVR) technique is used to estimate the capacitance value. Effectiveness of the technique depends on the training of SVR. Another technique based on the injection of low frequency voltage in dc-link and/or low frequency current in the ac side is suggested in [21]. The techniques suggested in[16]–[21], based on injection of low frequency voltage/current, lead to sub harmonics in the supply current. This may violate the limits mentioned in IEEE 519-2014 standard for a grid-feeding PV system [23]. To overcome this limitation, condition monitoring of an electrolytic capacitor for motor drive application is suggested in [22]. The inverter is modulated to inject a DC current in the motor just before the starting of the motor. The measurement of this current and dc-link voltage is used to determine the ESR. However, this technique is not applicable for online monitoring of electrolytic capacitor during the normal operation of the system and loads. IN addition to the research publication, there are various patents on the health monitoring of capacitor [24]–[26]. In [24],a method based on the pre-charging of the electrolytic capacitor via a charging resistor is discussed. The charging current and the voltage across the capacitor is used to determine the delay time of this RC circuit. This value is compared with a predefined constant, and the difference between them indicates the aging of the capacitor. This method may not be applicable for PV inverters, as the charging current for electrolytic capacitor would be provided by PV panels instead of the pre-charging resistor connected on the ac side. In [25], remaining lifetime of an electrolytic capacitor is determined based on the operating core temperature. The core temperature is estimated using the measured ambient temperature, its calculated power loss and suitable thermal model of the capacitor. Accuracy of this method may be limited due to errors in thermal and electrical modeling of the converter. In [26], a method based on the electrolytic capacitor voltage ripple is suggested. The voltage ripple is used as an indication of failure of the electrolytic capacitor. However, this method does not incorporate effects of variation in input voltage and temperature on the magnitude of voltage ripple. The aforementioned techniques either utilize additional circuits/sensors or require special operating conditions to determine the ESR and capacitance of the electrolytic capacitor. Further, the failure criterion based on the values of ESR or capacitance needs to be defined. This criterion may not optimize the profit generated from the grid-feeding PV system. For instance, in the case of delayed replacement of an electrolytic capacitor, PEE would reduce, thereby decreasing the earnings. IN the other case, early replacement of capacitor would increase the total cost of the PV system, which would also decrease the earnings. To address the aforementioned limitations, a technique for online health monitoring of electrolytic capacitor in PV inverter to minimize the payback period is proposed in [27]. However, the technique is not validated by detailed mathematical analysis or experimentation. Further, the effects of temperature and solar radiation on the performance of the technique were not discussed. A detailed comparison of the existing techniques with the proposed technique is shown in Table I. Most of the existing methods considered electrolytic capacitors to be unusable when ESR or capacitance value reaches to a critical value. However, in this paper a novel method to compare and analyze the remaining life of capacitor based on PEE is proposed. This method aims to maximize the revenue generated from the system. This technique allows continuous monitoring of PEE and suggests replacement of capacitor based on a critical value of PEE. Mathematical analysis using double Fourier series analysis (DFSA) is carried out to determine relation of PEE to the capacitance and ESR values. Further, the critical value of PEE is determined, at which replacement of electrolytic capacitor would lead to maximum earnings from the system. The effect of variation in temperature and solar radiation on the performance of the technique is discussed. A scaled-down laboratory prototype is developed to validate the proposed scheme. Results are discussed in this paper. The proposed method is implemented by using existing feedback signals used for MPPT controller, thereby avoiding additional cost. Further, this technique does not require special operating condition unlike few other techniques suggested in the literature. PEE can be used as a key performance indicator for fault diagnosis in a large grid-feeding PV system. This can be done by using data driven approaches or improved partial least-squares (PLS) used for health monitoring for the industrial applications [28], [29].The paper is organized as follows. In Section II, proposed technique is presented. The criterion for the replacement of capacitor is also discussed in this section. Section III covers the mathematical modeling of the technique. Detailed simulation studies are carried out and results are included in Section IV. The critical value of PEE at which capacitor could be replaced is also determined in this section. Further, practical aspects, including the effect of solar radiation and operating temperature

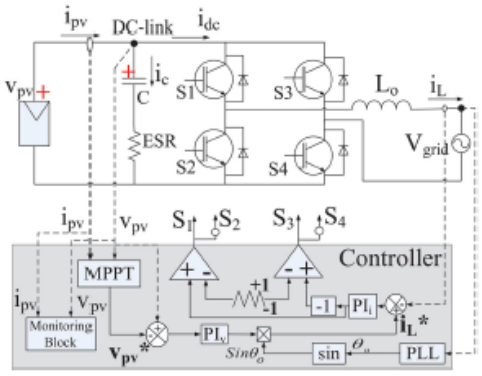


Fig. 1.Single-phase grid-feeding PV system.

results are presented in Section V. Section VI concludes the paper.

## II. PROPOSED TECHNIQUE

The proposed technique is divided into two sub modules: a)PEE calculation and b) criterion for replacement of capacitor.

### A. Power Extraction Efficiency (PEE) Calculation

Fig. 1 shows a single phase full bridge inverter, interconnecting to the grid. The controller includes MPPT

module, which generates the reference PV voltage. This voltage is realized using voltage and current controllers. DC-link voltage of this single phase inverter oscillates at twice the grid frequency($\omega o$). As this voltage is seen by the PV panel, the power supplied from the PV panel also oscillates with the same frequency. In the proposed technique, the ratio of average PV power over a time period of $\pi/\omega o$ to its maximum value is calculated to find the PEE. This is realized by the calculation of instantaneous power from the sampled values of PV voltage (*vpv*) and current (*ipv*).

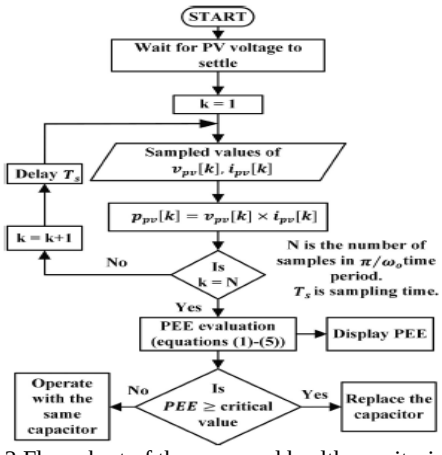


Fig. 2.Flow chart of the proposed health monitoring technique.

Reference value of PV voltage changes periodically to track the maximum power. The actual PV voltage follows its reference value with some delay. Therefore, the samples of PV voltage and current signals are taken after settling of PV voltage to its new reference value. A flow chart of the proposed technique is shown in Fig. 2. To address the above issue, sampling of $v_{pv}$and $i_{pv}$is done after settling of PV voltage, as shown in the first step of the flowchart. In next step, $k_{th}$ sample of $v_{pv}$and $i_{pv}$,$v_{pv}[k]$ and $i_{pv}[k]$,respectively, are sampled, where $k = 1, 2, \ldots, N$ and $N$ is the total number of samples in a time period of $\pi/\omega_o$. Then, $p_{pv}[k]$,$k$th sample of instantaneous PV power (*ppv*) is calculated from *vpv*[*k*] and *ipv*[*k*]. In the next step, average PV power *Pav*is calculated by

$$P_{av} = \sum_{K=1}^{N} P_{PV}[k] \backslash N (1)$$

Due to noise in measurement, the direct extraction of maximum power ($P_{max}$) from all the samples of $p_{pv}$ may not be accurate. To eliminate this effect, maximum power is calculated using the following method. The RMS power is calculated by

$$P_{rms}^2 = \sum_{K=1}^{N} (P_{PV}[k])^2 \backslash N (2)$$

$$p_{ripp,rms} = \sqrt{p_{rms}^2 - p_{av}^2} (3)$$

The maximum value of PV power is given by

$$p_{max} = \sqrt{2} \times p_{ripp,rms} + p_{av} (4)$$

The ratio of average PV power to the maximum PV power is PEE

$$\text{PEE} = \frac{P_{av}}{P_{max}} (5)$$

Equations (1)–(5) are implemented in the PEE evaluation block of the flowchart shown in Fig. 2. The flowchart shown in Fig. 2 is the part of the monitoring block as shown in Fig. 1.Estimated PEE value is compared with the critical value of PEE and decision is made whether to replace the capacitor or not. This critical value of PEE is calculated using the criterion for replacement of capacitor based on PEE, which is discussed in the subsequent section.

**B. Criterion for Replacement of Capacitor**

The degradation of an electrolytic capacitor results in larger dc-link voltage ripples due to which average PV power decreases. The reduced PEE results in lower earnings from the PV system. Therefore, timely replacement of the capacitor is required. However, frequent replacement of the capacitor will add to the system cost, which may decrease the earnings. Therefore, method to determine the critical value of PEE ($PEE_{cr}$) at which the capacitor should be replaced is shown in Fig. 3. The first step involves determination of PEE(t) as the capacitor degrades with time. This analytical equation can be determined either by using simulation studies with a suitable capacitor degradation model or by performing experimentation based on the accelerated aging of the capacitor. In the flow chart, PEE(t) (PEE at instant t) is calculated using the analytical equation and compared with the critical value. If calculated PEE(t) is less than PEE*cr* , incremental revenue ($\Delta r$) per hour is calculated using the following equation:

$$\Delta r = (PEE\ (t) \times P_{PV,max} \times n\ MPPT \times nconv) \times FIT (6)$$

where *PP V*,$_{max}$is the maximum possible PV power in *t*th hour(in kW), $\eta$ *MP P T*is the extraction efficiency of the MPPT algorithm, $\eta conv$ is the power conversion efficiency of the inverter and FIT is feed in tariff (in $/kWh). This new value of revenue is added to the previously calculated revenue. The time is updated by 1 h and the process of revenue calculation is repeated until PEE reduces to PEE*cr*. At this instant, the capacitor is changed

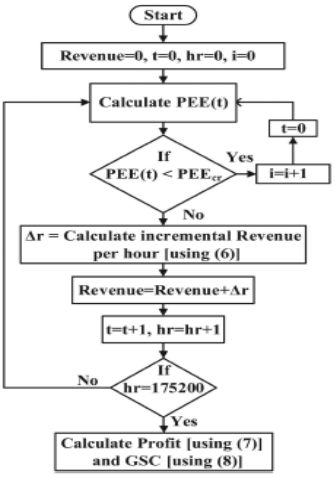

Fig. 3. Flowchart for profit calculation.

Now again the process of revenue calculation is repeated for the new capacitor. This process is repeated until 20 years, i.e., 175 200 h. Profit generated by this system in its lifetime(20 years) is calculated using Profit = Revenue (in 20 years) - Gross System Cost (7) where the gross system cost (GSC) is calculated by GSC = PV system cost + *i* ×capacitor replacement cost (8) where *i* is the number of replaced electrolytic capacitors in20 years. The replacement cost of the capacitor includes the cost of a new capacitor, labor cost, and revenue loss due to the shutdown of the inverter [30]. Using the flowchart shown in Fig. 3, profit for a specific value $PEE_{cr}$ is found. By repeating this process for various values of $PEE_{cr}$, a plot for profit generated from the system in its lifetime (20 years) for different values of critical PEE is obtained. Detailed simulation results to obtain this plot are provided in Section IV-B. The maximum value of this curve would indicate the critical value of PEE at which the capacitor should be replaced.

## III. CONTROL DESIGN

### A. Harmonics Components in PV Voltage

The analytical equation for PEE versus ESR and C is derived for the single phase grid connected PV system. The full bridge inverter, shown in Fig. 1, is operated by a unipolar sinusoidal pulse width modulation switching scheme, as shown in Fig. 4.DC-link voltage ($v_{pv}$) and current ($i_{dc}$) include oscillations of twice the grid frequency ($\omega_o$) and the switching frequency ($\omega_c$).Therefore, DFSA is used to determine various harmonic components. By using double Fourier series, any periodic function of two variables is expressed, as summation of sinusoidal components whose frequencies are ($m\omega c$+ $n\omega o$), where *m* is a nonnegative integer and *n* is an integer. The integer s*m* and *n* are called the carrier index and the fundamental index, respectively.

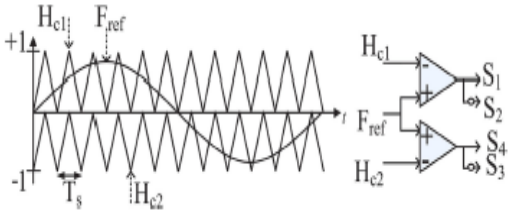


Fig. 4.Unipolar PWM switching scheme.

Using DFSA, dc-link current *idc* is expressed as [31]

$$i_{dc}(\omega_0 t, \omega_c t) = \frac{\vec{C_{00}}}{2} + \sum_{m=0}^{\infty} \sum_{n=-\infty}^{\infty} \vec{C_{mn}} [\sin(m\omega_c t + n\omega_c t + \vec{C_{mn}}] \quad (9)$$

(m=n)≠ 0

Where *Cmn*| and ∠−−→*Cmn* are the magnitude and the phase of the (*mωc*+ *nωo*) frequency component in the dc-link current, which are given by

$$\vec{C_{mn}} = \frac{1}{2\pi^2} \int_{-\pi}^{\pi} \int_{-\pi}^{\pi} i_{dc}(t) e^{j(m\omega_e + n_{\omega 0})t} \mathrm{d}(\omega_c t) d(\omega_0 \mathrm{t}) \quad (10)$$

To find the values of |−−→*Cmn*| and ∠−−→*Cmn*, instantaneous dc-link current is determined using [32]

$$i_{dc} = i_L(S_1S_4 - S_2S_3) \quad (11)$$

Where *iL* is the inductor current given by *iL= IL* sin(*ωot* −*φ*)and S1–S4 are the states of the semiconductor switches. To determine the switch states, following equations of carrier *Hc*1and *Hc*2 and reference waveform *Fref* are used:

$$H_{c1}(\omega_c t) = \begin{cases} -\omega_c t/\pi, & \text{for } -\pi < \omega_c t < 0 \\ \omega_c t/\pi, & \text{for } 0 < \omega_c t < \pi \end{cases}$$

$$H_{c2}(\omega_c t) = \begin{cases} -\omega_c t/\pi - 1, & \text{for } -\pi < \omega_c t < 0 \\ \omega_c t/\pi - 1, & \text{for } 0 < \omega_c t < \pi \end{cases}$$

$$F_{\text{ref}}(\omega_o t) = M \sin(\omega_o t)$$

Where *M* is the modulation index. By using (11) and (12), the conditions for *id c*are tabulated in Table II. Contour plot describing the boundary conditions for *idc* is shown in Fig. 5.The various frequency components in dc-link current (−−→*Cmn*) are found by solving the double integral equation (10), along with the boundary conditions determined in Table II. These current components are absorbed by the dc-link capacitor due to its low impedance as compared to the PV panel at the corresponding

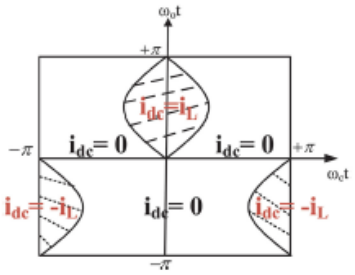


Fig. 5. Contour plot of *idc*.

frequencies. Therefore, the ($m\omega c$+ $n\omega o$) harmonic component in the voltage across the dc-link capacitor (−−→$V_{mn}$) is given by the product of the corresponding current component and the impedance offered by the capacitor at that frequency

$$\vec{V_{mn}} = \vec{C_{mn}}\{ESR + \frac{1}{J(m\omega_c + n\omega_0)C} \quad (12)$$

Summation of all these harmonic components in the PV voltage(_*vpv*) is given by

$$v_{pv} = \frac{\vec{C_{00}}}{2} + \sum_{m=0}^{\infty} \sum_{n=-\infty}^{\infty} \vec{v_{mn}} [\sin(m\omega_c t + n\omega_0 t + \vec{v_{mn}}] \quad (13)$$

(m=n)≠ 0

Addition of all AC components present in PV voltage determined from (14) would be used later along with the PV model to determine the effect of C and ESR on PEE.

**B. PV Model**

Instantaneous PV current (*ipv*) for ideal PV array is

$$i_{pv} = I_g + I_0(1 - e^{v_{pv}\backslash nv_T n_s}) \text{ (14)}$$

Where *Ig* and *Io* are light generated and diode reverse saturation currents, respectively. *Vpv* is instantaneous PV voltage, *η*is ideality factor, *VT* is thermal voltage, and *ns* are the number of solar cells in series. At MPP,

$$i_{MPP} = I_g + I_0(1 - e^{v_{MPP}\backslash nv_T n_s}) \text{ (15)}$$

Where $I_{MPP}$ and $V_{MPP}$ are the PV current and voltage, respectively, at MPP. Writing the second-order approximate Taylor series for $i_{pv}$ at MPP using (15) and (16) [33]

$$i_{pv} = I_{MPP} + (\partial I_{MPP}/\partial I_{MPP})(V_{PV} - V_{MPP}) + (1/2)(\partial^2 I_{MPP}/\partial v_{MPP}^2)(v_{pv} - v_{MPP})^2 \text{ (16)}$$

After expanding and rearranging (17)

$$i_{pv} = Av_{pv}^2 + Bv_{pv} + D \text{ (17)}$$

where constants

$$A = \frac{1}{2}\frac{\partial^2 I_{MPP}}{\partial V_{MPP}^2}, B = \frac{\partial I_{MPP}}{\partial V_{MPP}} - V_{MPP}\frac{\partial^2 I_{MPP}}{\partial V_{MPP}^2}$$

$$\text{and, } D = \frac{1}{2}\frac{\partial^2 I_{MPP}}{\partial V_{MPP}^2}V_{MPP}^2 - V_{MPP}\frac{\partial I_{MPP}}{\partial V_{MPP}} + I_{MPP}.$$

$$i_{pv} = A(V_{MPP} + V_{PV})^2 + B(V_{MPP} + V_{PV}) + D \text{ (17)}$$

C. Effect of ESR and C on PEE

The instantaneous PV power is given by $p_{pv}(t) = v_{pv}i_{pv}$. Substituting, $v_{pv} = V_{MPP} + \_v_{pv}$ and $i_{pv}$ from (19) and rearranging

$$P_{pv}(t) = AV_{MPP}^3 + BV_{MPP}^2 + DV_{MPP} + A(V_{PV}^3 + 3v_{MPP}V_{PV}^2 + 3V_{MPP}^2V_{PV}) + B(V_{PV}^2 + 2V_{MPP}V_{PV}) + DV_{pv}$$

The average PV power ($P_{av}$) over a second harmonic time period($\pi/\omega_o$) is given by

$$P_{av} = \frac{1}{\pi/\omega_0}\int_t^{t+(\pi/\omega_0)} p_{pv(t)dt} \text{ (18)}$$

$\backslash p_{pv}$ and $\_v_{pv}$ are substituted from (20) and (14), respectively. The integration of terms such as $_vp_{v3}$and$v_{pv}$, over the time period ($\pi/\omega_o$) is zero because these terms only have sinusoidal components whose frequencies are integral multiple of $2\omega_o$

$$P_{av} = P_{MPP} + \frac{1}{2}(3V_{MPP}A + B)\sum_{m=0}^{\infty}\sum_{n=-\infty}^{\infty}[\vec{v_{mn}}]^2 \text{ (19)}$$

Where $P_{MPP} = I_{MPP} \times V_{MPP}$. Substituting $P_{av}$ from (22) in(5) gives the PEE due to oscillations in PV voltage as

$$\text{PEE}=1+\frac{3v_{MPP}A+B}{2P_{MPP}}\sum_{m=0}^{\infty}\sum_{n=-\infty}^{\infty}|\vec{V_{mn}^2}| \text{ (20)}$$

$$PEE = 1 + \frac{3V_{MPP}A+B}{2P_{MPP}}.\sum_{m=0}^{\infty}\sum_{n=-\infty}^{\infty}\vec{c_{mn}^2}\,(ESR^2 + \frac{1}{m\omega_e+n\omega_0)C})^2$$

(m=n)≠ 0 (21)

This equation determines the effect of the values of ESR and C on the PEE. Results from this derived equation are compared with the simulation results in Section IV-A.

## IV. SIMULATION RESULTS AND DISCUSSION

**A. Simulation Results**

A single phase grid feeding PV inverter along with the controller, shown in Fig. 1, is simulated in the MATLAB/Simulink platform. Specifications of a simulated PV system and inverter components are given in Table III. The dc-link capacitor is selected in order to ensure that the low-frequency (twice the grid frequency) voltage ripple at full power is less than 10% [9]. The capacitor selected for the simulation studies is EPCOS B43544 (330 $\mu$F, 500 V). The perturb and observe (P&O) MPPT technique is used to determine the reference voltage signal, which is realized using inner voltage and current controllers as shown

TABLE I
SPECIFICATIONS OF SIMULATED SYSTEM

| Parameter | Variable | Value |
|---|---|---|
| Maximum Power | $P_{MPP}$ | 2 kW |
| Voltage at $P_{MPP}$ | $V_{MPP}$ | 384 V |
| Current at $P_{MPP}$ | $I_{MPP}$ | 5.208 A |
| Light generated current | $I_g$ | 6.446 A |
| Open-circuit voltage | $V_{OC}$ | 500 V |
| Grid frequency | $f_0$ | 50 Hz |
| Grid Voltage | $V_{grid}$ | 230 V |
| Inductor | $L$ | 3 mH |
| DC-link Capacitor | C | 330 $\mu$F |
| ESR of input Cap. | ESR | 0.210 Ω |
| Switching frequency | $f_s$ | 10 kHz |

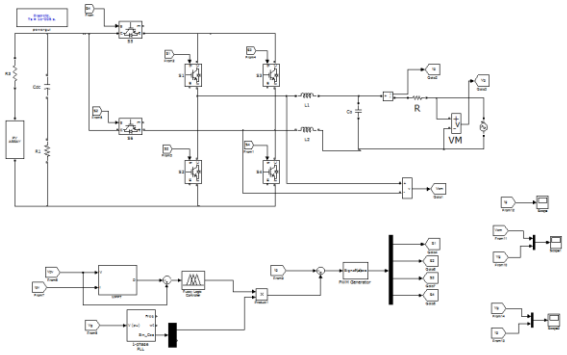

Fig 6 Simulink Model of the Proposed Grid Connected PV-Improved H6 Inverter

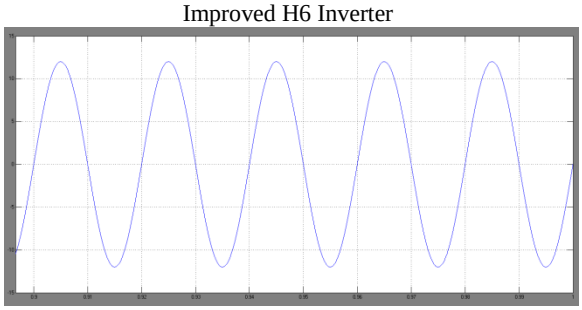

Fig. 7. (a) Simulink waveforms of the Grid Feeding Inverter Current

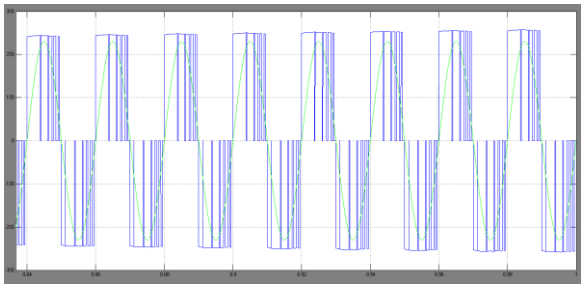

Fig. 8. (a) Simulink waveforms of the PWM inverter voltage and grid voltage

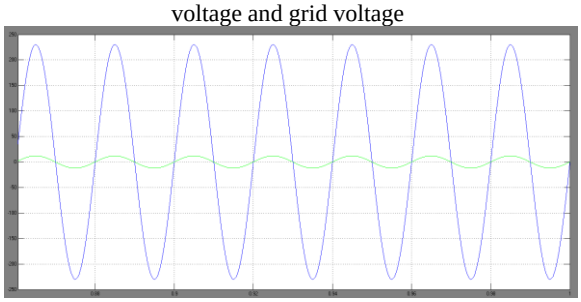

Fig. 9. (a) Simulink waveforms of GRID Feeding Voltage & Current

The inverter pulse width modulated (PWM) voltage, grid voltage, and current are shown in Fig. 6. With aging ESR and C changes, as per the relationships discussed in [34]. Due to reduction in C and increase in ESR with time, PEE is expected to decrease. The proposed technique shown in Fig. 2 is implemented along with the inverter in Simulink. The sampling rate (1/*Ts*) is the same as the switching frequency (*fs*). Simulation results of the proposed technique along with the results determined from the mathematical model. From the results it is observed that, as the capacitor degrades, PEE deteriorates. The values of the extraction efficiency predicted from the mathematical model are slightly higher than that determined by simulation. This is mainly because of two factors. First, the solar PV model used in the mathematical prediction is approximated by using Taylor series. Second, the mathematical model does not incorporate the no idealities of the system, such as switch resistance, diode resistance, inductor resistance, etc., which would modify the ripple component in solar PV current and voltage. Therefore, the PEE determined by simulation are more accurate as compared to that determined by mathematical modeling. However, the small magnitude of error justifies the effectiveness of the developed mathematical model. Further, for predictions using Simulink model, root mean square error (RMSE) = 1.0721 × 10−8 and for predictions using mathematical model RMSE= 2.4939 × 10−6. From RMSE of each method, it can be clearly observed that the predictions of the Simulink model are more accurate as compared to the mathematical model.

## VI. CONCLUSION

A technique was suggested in this paper for online health monitoring of an electrolytic capacitor for a single phase PV system. The proposed technique is limited to only single stage single phase grid connected PV inverters. Following are the key conclusions. Degradation of electrolytic capacitor leads to rise in dc link voltage ripples. Larger magnitude of dc-link voltage ripples reduces the average PV power extracted from PV, thereby reducing PV PEE. Replacement of the capacitor is suggested on the basis of PEE to maximize earnings from the PV system in20 years. Detailed steps involved in determination of the critical value of PEE for which the capacitor should be replaced are included in this paper. Mathematical modeling of the system is performed using DFSA. The analytical equation relating the PEE with C and ESR values is derived. Detailed simulation studies are carried out to verify the efficacy of the scheme. Practical issues that could affect the performance of the proposed technique are discussed. It is found that the value of PEE does not change significantly with the variation in solar radiation and operating temperature. To check the viability of the scheme, experimental studies are performed using a laboratory prototype developed for this purpose. PEE, found using the proposed technique, decreases with reduction in C and increase in ESR values. The values found using experimentation is in agreement to those obtained from simulation of the same system. The key advantage of the proposed technique is that no additional circuits or sensors are required for online health monitoring of the electrolytic capacitor. The sensors used for MPPT algorithms are sufficient to realize the proposed monitoring scheme. Further, proposed technique offers online health monitoring of the electrolytic capacitor.

## REFERENCES

[1] J. Carrasco *et al.* “Power electronic systems for the grid integration of renewable energy sources: A survey,” *IEEE Trans. Ind. Electron.*, vol. 53,no. 4, pp. 1002–1016, Apr. 2006.

[2] P. Manganiello, M. Ricco, G. Petrone, E. Monmasson, and G. Spagnuolo,“Optimization of perturbative PV MPPT methods through online system identification,” *IEEE Trans. Ind. Electron.*, vol. 61, no. 12, pp. 6812–6821, Dec. 2014.

[3] J. S. C. M. Raj and A. E. Jeyakumar, “A novel maximum power point tracking technique for photovoltaic module based on power plane analysis of I-V characteristics,” *IEEE Trans. Ind. Electron.*, vol. 61, no. 9, pp. 4734–4745, Sep. 2014.

[4] M. A. G. de Brito, L. Galotto, L. P. Sampaio, G. de Azevedo e Melo, andC. A. Canesin, “Evaluation of the main MPPT techniques for photovoltaic applications,” *IEEE Trans. Ind. Electron.*, vol. 60, no. 3, pp. 1156–1167,Mar. 2013.

[5] N.D. Benavides and P. L. Chapman, “Modeling the effect of voltage rippleon the power output of photovoltaic modules,” *IEEE Trans. Ind. Electron.*,vol. 55, no. 7, pp. 2638–2643, Jul. 2008.

[6] M. Bramoulle, “Electrolytic or film capacitors?,” in *Conf. Rec. 33rd IEEEIAS Annu. Meet.*, St. Louis, MO, USA, Oct. 1998, vol. 2, pp. 1138–1141.

[7] M. L. Gasperi, “Life prediction modeling of bus capacitors in AC variable frequency drives,” *IEEE Trans. Ind. Appl.*, vol. 41, no. 6, pp. 1430–1435,Nov./Dec. 2005.

[8] C. R. Sullivan, J. J. Awerbuch, and A. M. Latham, “Decrease in photovoltaic power output from ripple: Simple general calculation and the effect of partial

shading," *IEEE Trans. Power Electron.*, vol. 28, no. 2,pp. 740–747, Feb. 2013.
[9] S. Zengin, F. Deveci, and M. Boztepe, "Decoupling capacitor selection inDCMfly back PV micro inverters considering harmonic distortion,"*IEEETrans. Power Electron.*, vol. 28, no. 2, pp. 816–825, Feb. 2013.
[10] K. Harada, A. Katsuki, and M. Fujiwara, "Use of ESR for deterioration diagnosis of electrolytic capacitor,"*IEEE Trans. Power Electron.*, vol. 8,no. 4, pp. 355–361, Oct. 1993.
[11] Y. M. Chen, H. C. Wu, M. W. Chou, and K. Y. Lee, "Online failure prediction of the electrolytic capacitor for LC filter of switching-mode power converters," *IEEE Trans. Ind. Electron.*, vol. 55, no. 1, pp. 400–406, Jan. 2008.
[12] A. Lahyani, P. Venet, G. Grellet, and P. J. Viverge, "Failure predictionof electrolytic capacitors during operation of a switch modepower supply," *IEEE Trans. Power Electron.*, vol. 13, no. 6, pp. 1199–1207,Nov. 1998.
[13] H. M. Pang and P. M. H. Bryan, "A life prediction scheme for electrolytic capacitors in power converters without current sensor," in *Proc. IEEEAppl. Power Electron. Conf. Expo.*, Palm Springs, CA, USA, Feb. 2010, pp. 973–979.
[14] E. C. Aeloiza, J. H. Kim, P. N. Enjeti, and P. Ruminot, "A real time method to estimate electrolytic capacitor condition in PWM adjustable speed drives and uninterruptible power supplies," in *Proc. 36th IEEEPower Electron. Spec., Conf.*, Recife, Brazil, Jun. 2005, pp. 2867–2872.
[15] M. A. Vogelsberger, T. Wiesinger, and H. Ertl, "Life-cycle monitoring and voltage-managing unit for DC-Link electrolytic capacitors in PWMconverters," *IEEE Trans. Power Electron.*, vol. 26, no. 2, pp. 493–503,Feb. 2011.
[16] D. Lee, K. Lee, J. Seok, and J. Choi, "Online capacitance estimation of DC-link electrolytic capacitors for three-phase AC/DC/AC PWMconverters using recursive least squares method," *Proc. Inst. Elect.Eng.—Elect. Power Appl.*, vol. 152, no. 6, pp. 1503–1508, Nov./Dec.2005.
[17] X. S. Pu, T. H. Nguyen, D. C. Lee, K. B. Lee, and J. M. Kim, "Fault diagnosis of DC-Link capacitors in three-phase AC/DC PWM convertersby online estimation of equivalent series resistance," *IEEE Trans. Ind. Electron.*, vol. 60, no. 9, pp. 4118–4127, Sep. 2013.
[18] T. Nguyen and D. Lee, "Deterioration monitoring of DC-link capacitors in AC machine drives by current injection,'